(This is a sample cover image for this issue. The actual cover is not yet available at this time.)

Journal of Theoretical Biology 305 (2012) 88–95

Contents lists available at SciVerse ScienceDirect

Journal of Theoretical Biology

journal homepage: www.elsevier.com/locate/yjtbi

Determinants of periodicity in seasonally driven epidemics

Asher Uziel *, Lewi Stone

Tel Aviv University Biomathematics Unit, Faculty Life Science, Tel-Aviv University, Ramt aviv, P.O. 39040, Israel

ARTICLE INFO

Article history:
Received 8 December 2010
Received in revised form
23 February 2012
Accepted 29 February 2012
Available online 23 March 2012

Keywords:
Seasonal epidemics
Infectious diseases
Nonlinear dynamics
SIR model

ABSTRACT

Seasonality strongly affects the transmission and spatio-temporal dynamics of many infectious diseases, and is often an important cause for their recurrence. However, there are many open questions regarding the intricate relationship between seasonality and the complex dynamics of infectious diseases it gives rise to. For example, in the analysis of long-term time-series of childhood diseases, it is not clear why there are transitions from regimes with regular annual dynamics, to regimes in which epidemics occur every two or more years, and vice-versa. The classical seasonally-forced SIR epidemic model gives insights into these phenomena but due to its intrinsic nonlinearity and complex dynamics, the model is rarely amenable to detailed mathematical analysis.

Making sensible approximations we analytically study the threshold (bifurcation) point of the forced SIR model where there is a switch from annual to biennial epidemics. We derive, for the first time, a simple equation that predicts the relationship between key epidemiological parameters near the bifurcation point. The relationship makes clear that, for realistic values of the parameters, the transition from biennial to annual dynamics will occur if either the birth-rate (μ) or basic reproductive ratio (R_0) is increased sufficiently, or if the strength of seasonality (δ) is reduced sufficiently. These effects are confirmed in simulations studies and are also in accord with empirical observations. For example, the relationship may explain the correspondence between documented transitions in measles epidemics dynamics and concomitant changes in demographic and environmental factors.

1. Introduction

Seasonality is a driving force that controls the transmission and spatio-temporal dynamics of many common infectious diseases (London and Yorke, 1973; Fine and Clarkson, 1982; Anderson and May, 1991; Smith, 1983; Pascual and Dobson, 2005; Altizer et al., 2006; Grossman et al., 1977; Stone et al., 2007; Begon et al., 2009). This is no better seen than in the historical long-term data sets of seasonally recurring childhood infectious diseases, such as measles, mumps, chickenpox, polio and pertussis (London and Yorke, 1973; Fine and Clarkson, 1982; Ward, 1944; Fine and Clarkson, 1986; Trevelyan et al., 2005). In their landmark study, Fine and Clarkson (Fine and Clarkson 1982; Fine and Clarkson, 1986) demonstrated that the seasonally changing contact rate between children, which sharply increases at the beginning of each school year, governs the recurrence of the childhood diseases outbreaks. Other patterns of seasonality, such as the case of polio where the disease transmission peaks during summer and autumn (Sharma, 2003), also appear to sustain recurrent epidemics (Grassly et al., 2006). Furthermore, model simulations and analysis of empirical data strongly suggest that relatively mild seasonality tends to induce annual outbreaks, while more intense seasonality induces biennial or even complex or chaotic dynamics (Fine and Clarkson, 1982; Stone et al., 2007; Fine and Clarkson, 1986; Aron and Schwartz, 1984; Olsen and Schaffer, 1990; Finkenstädt and Grenfell, 1998; Earn et al., 2000; Keeling et al., 2001). For example, polio generally occurs annually in India (Grassly et al., 2006), while measles has had a strong biennial component for some extended periods in London (Finkenstädt and Grenfell, 1998). Moreover, the same disease can have different temporal patterns during different epochs (Stone et al., 2007; Earn et al., 2000; Keeling et al., 2001; Finkenstädt and Grenfell, 2000). Remarkably, measles incidence time-series in the UK (measdata.html) (Fig. 1) shows transitions from a period with regular annual dynamics to an epoch in which epidemics occur every two or more years, and vice-versa.

The variations in the temporal pattern of epidemics may be viewed as a manifestation of chaotic dynamics, but might well also be due to changes in epidemiological factors such as population birth rate, magnitude of disease transmission, and strength of seasonality (Earn et al., 2000; Ferrari et al., 2008; Finkenstädt et al., 1998). However, the functional dependency of the inter-epidemic time on epidemiological parameters is still poorly understood. Our goal in this work is to deduce such a

* Corresponding author. Tel./fax: +972 3 6409806.
E-mail addresses: uziel@post.tau.ac.il (A. Uziel), lewi@post.tau.ac.il (L. Stone).

0022-5193/$ - see front matter © 2012 Elsevier Ltd. All rights reserved.
http://dx.doi.org/10.1016/j.jtbi.2012.02.031

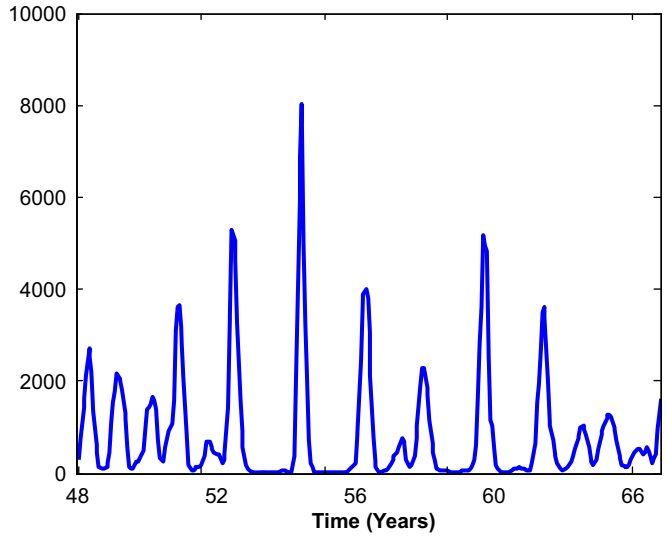

Fig. 1. Time series of reported measles infectives (monthly) from Birmingham, UK (measdata.html). Prevaccine epidemics dynamics shows transitions from a period with regular annual dynamics to periods with more complex dynamics, and vice-versa.

mathematical relationship, and use it to better comprehend the mechanism of transition from annual to multi-annual epidemic dynamics.

To this end we study the seasonally forced SIR (Susceptible, Infectious, Recovered) epidemic model (Kermack and McKendrick, 1927). The model assumes that individuals who have recovered from a disease gain life-long immunity against the infection, as is reasonable for many childhood diseases. The relative simplicity of the SIR model and the fact that it captures many key aspects of childhood-diseases spread, have made it a popular candidate in the modeling of these diseases (Earn et al., 2000; Keeling et al., 2001; Keeling and Rohani, 2007).

Unfortunately, in the presence of seasonal forcing, the oscillatory dynamics of the SIR model are generally complex and rarely amenable to mathematical analysis (Keeling and Rohani, 2007). Nevertheless, progress was recently made in this direction after employing several simplifying approximations (Stone et al., 2007; Olinky et al., 2008). It was found that given the number of susceptibles left after a major epidemic (S_0), it is possible to predict the occurrence of either an epidemic outbreak next year, or a '*skip*'—a year in which an epidemic fails to initiate. If S_0 is above a critical value (defined as S_c), an epidemic outbreak is expected in the subsequent year, otherwise a skip. However, this method requires knowledge of S_0, which is not a parameter of the model and is difficult to measure in practice.

Here we have made use of the framework of Stone et al. (2007) and Olinky et al. (2008) for studying seasonally forced models especially with relation to S_0. We modify and extend their work in a manner that allows calculating the threshold (bifurcation) points for a switch from annual to biennial epidemics as a function of the model parameters alone. We show the threshold criteria systematically explain various empirical observations and analytical results that pertain to epidemics dynamics of childhood infectious diseases.

2. Results

2.1. The seasonally forced SIR model

SIR models (Keeling and Rohani 2007) assume that, from an epidemiological point of view, a population can be divided into three classes: susceptible (S), infected (I) and recovered/removed (R). The model describes the process of disease spread from infected individuals to those that are susceptible. Infected individuals eventually recover from the disease and are assumed to have acquired long-term immunity, and are 'Removed' from the process as they can neither infect nor be infected. The rate of transition from S to I is, assuming a homogenously mixing population, a first order collision term between the number of infected and the number of susceptible and thus proportional to the product SI. In the *seasonally* forced SIR model, the transition rate also depends on the seasonal driver, and the equations are given by:

$$\frac{dS}{dt} = \mu(1-S) - \beta(t)IS, \tag{1.1}$$

$$\frac{dI}{dt} = \beta(t)IS - (\gamma+\mu)I. \tag{1.2}$$

In these equations, S and I represent proportions of the total population (i.e., $S+I+R=1$). The mean infection time of the disease is given by $1/\gamma$. To maintain a constant population, the birth rate μ is set equal to the mortality rate. The transition-rate from S to I is set by the parameter $\beta(t)$ and incorporates time-dependent external factors affecting the contact rate between members of the population and the infectivity of the disease. An annual sinusoidal forcing is commonly employed (London and Yorke 1973; Aron and Schwartz 1984; Olsen and Schaffer 1990):

$$\beta(t) = \beta_0(1+\delta\sin\omega t), \tag{1.3}$$

where β_0 is the average transmission rate-constant, δ is the strength of the seasonality and ω is set for a period of one year. However, such a forcing term might not be appropriate for childhood diseases where the time-dependent transmission changes abruptly upon initiation and termination of the school-term. Another approach is to use a term-time forcing whereby β is relatively high (β_+) and constant for the school-term and relatively low (β_-) and constant during all holiday periods in the year (Keeling et al., 2001; Keeling and Rohani, 2007; Bolker and Grenfell, 1993). An intermediate method between these two approaches is to model seasonality as a "square-wave" (Altizer et al., 2006; Olinky et al., 2008) such that β_+ is for half of the year (*Hi-Season*) and β_- during the other half (*Lo-Season*). That is,

$$\beta(t) = \begin{cases} \beta_+ \equiv \beta_0(1+\delta), & 0 \le (t \mod 1) < 0.5 \\ \beta_- \equiv \beta_0(1-\delta), & 0.5 \le (t \mod 1) \end{cases}, \tag{1.4}$$

where t is the time in units of years. Thus over time the seasons changes sequentially $Hi \to Lo \to Hi \to \ldots$ The square-wave approximation simplifies the analysis and yet the dynamics are nevertheless similar to either sinusoidal forcing or term-time forcing (Altizer et al., 2006; Olinky et al., 2008).

2.1.1. The biphasic SIR (B-SIR) model

This section is divided into two parts. In the first part we suggest that SIR dynamics can be regarded as alternating between (i) a relatively fast epidemic phase in which there is a significant increase in the number of infected as well as a rapid decrease in the number of susceptibles and (ii) a slow build-up phase in which there is a continuous replenishment of susceptibles. We show that in each of these two phases the SIR equations can be approximated in a simpler form. In the second part we present the B-SIR (Biphasic SIR) model which relies on this approximation and is constructed to mimic SIR dynamics on a multiennial epidemic cycle. This allows determination of the threshold (bifurcation) values at which there is transition from biennial to annual epidemic dynamics.

2.1.1.1. Forced SIR dynamics: alternating between epidemic and build-up phases. Our work is guided by a recent analysis of the forced SIR model (Olinky et al., 2008). We focus on SIR dynamics in the parameters range commonly documented for measles dynamics (i.e., $R_0=10\ldots 20$, $\mu=0.01\ldots 0.03$) (Anderson and May, 1991; Keeling and Rohani, 2007). Fig. 2A depicts a typical simulation of the model (Eqs.1) in the biennial regime. The figure shows an epidemic in the first year, characterized by a marked rise in the number of infected that is succeeded by a rapid decline in the number of susceptibles, until the epidemic itself dies out. In the second year the epidemic attempts to trigger but is curtailed due to the seasonal change ($Hi\rightarrow Lo$) and fails to take-off. Instead, there is a *skip*. Superimposed on the figure is the square wave transmission-rate forcing $\beta(t)$, demonstrating how the seasonal change is associated with the curtailing. The biennial dynamics is better viewed in the phase-plane diagram (Fig. 2B) where the log of infective numbers (log I) is plotted as a function of susceptible numbers. The model's trajectory rotates counter-clockwise in the S-Log(I) plane. The epidemic, which occurs every two years, is portrayed in the upper-half of the phase plane where infectives pass through a maximum. The lower half of the phase plane corresponds to skip dynamics, which is characterized by a continuous increase in the number of susceptibles, despite the local peak in infectives.

We thus define in this work the *build-up phase* as the time-duration where the number of susceptibles continuously increases, and the *epidemic phase* as the period where the number of susceptible continuously decreases while infectives pass through a maximum (see Fig. 2B). We emphasize that, unlike other definitions, we characterize the onset of the epidemic phase by the point where susceptibles start to fall and not where infective start to increase, because, as exemplified by the skip shown in Fig. 2, an increase in infectives does not always lead to an epidemic. The forced SIR model dynamics can consequently be viewed as an alternating series of build-up phases and epidemic phases.

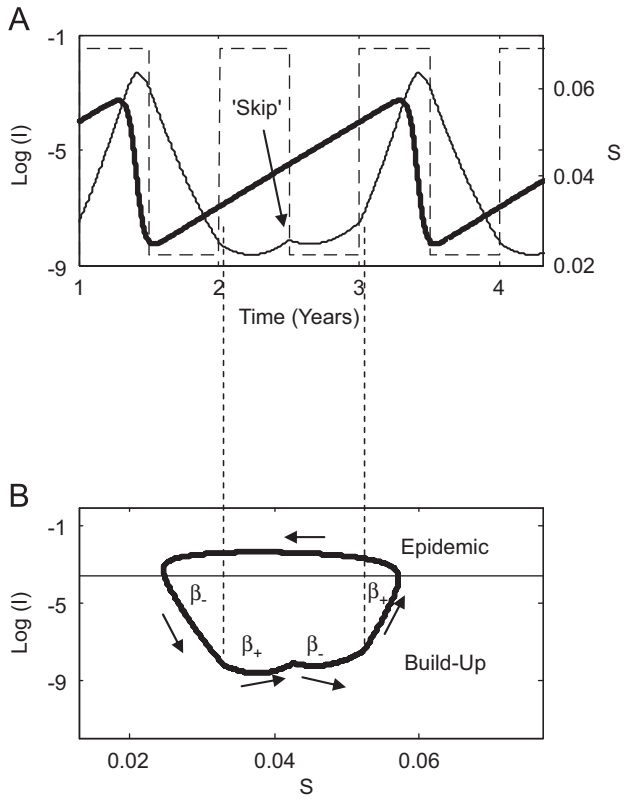

Fig. 2. Visualization of the build-up and epidemic phases: forced SIR model time-series together with the associated phase-plane trajectory, for a biennial epidemic cycle. (A) A representative 3-years time-series simulation of infectives (ordinary line) and susceptibles (thick line). The seasonally-forced transmission-rate parameter $\beta(t)$ (dashed line) is superimposed. Parameters values used here: $\beta_0=1600$ per year, $\delta=0.095$, $\gamma=66$ per year, $\mu=0.02$ per year (B) Phase plane diagram with the number of infectives log(I) plotted as a function of susceptible number (S), corresponding to the time-series. The trajectory of the model rotates counter-clockwise around the phase-plane.

The forced SIR model equations may be approximated as follows for each of the two phases. During the *epidemic phase* birth/death events have little influence on the population compared to the ongoing outbreak. Thus, when $\mu \ll \beta(t)IS$, Eqs. (1) reduce to (Olinky et al., 2008)

$$\frac{dS}{dt}=-\beta(t)IS,\quad \frac{dI}{dt}=\beta(t)IS-\gamma I. \tag{2.1}$$

The *build-up phase* occurs after an epidemic so that the number of infectives is relatively small. Therefore, when $\mu \gg \beta(t)IS$, Eqs. (1) can be approximated (see Methods) as (Olinky et al., 2008)

$$\frac{dS}{dt}=\mu(1-S),\quad \frac{dI}{dt}=\beta(t)IS-(\gamma+\mu)I. \tag{2.2}$$

Under this approximation $S(t)$ is described by

$$S(t)=1-(1-S_0)e^{-\mu t}, \tag{2.3}$$

where S_0 is the number of susceptible just after an epidemic, at the initiation of the build-up phase. To allow for the subsequent analytical derivation, we can simplify (2.3) by considering that $\{S_0, (\mu t)\} \ll 1$ (see Methods). The time evolution of the susceptibles during the build-up phase can thus be approximately described as (Olinky et al., 2008):

$$S(t)=S_0+\mu t. \tag{2.4}$$

2.1.1.2. B-SIR model details. The B-SIR model approximates forced SIR dynamics by separately considering the dynamics during the build-up and epidemic phases, and sensibly connecting the phases one after the other. Specifically, the model mimics an n-year stable periodic solution (or "*cycle*") where the phase-plane trajectory closes upon itself every n years such that one year has an epidemic and $(n-1)$ years are 'skips'. Fig. 3A and B depict an example of a 2-year biennial cycle, with alternation between an epidemic year and a skip. The B-SIR model is sketched in Fig. 3C.

We construct a map between S_0, defined as the number of susceptibles in the population just after the current epidemic phase, to S_1, the susceptible number just before the next epidemic phase. Similarly we construct a map from S_1 to S'_0 immediately after the next epidemic phase. Composing the two maps together, results in the map $S_0\rightarrow S'_0$ between S at the conclusion of the current epidemic phase to S at the end of the subsequent epidemic (Fig. 3). Finally, applying the closure condition for a cycle $S_0=S'_0$, it becomes possible to determine the feasible range of parameters-values for a cycle of any specified period.

The model reconstructs the dynamics on an n-year limit cycle as follows. We begin with the build-up phase and assume that the time spent in the build-up phase during an n-year epidemic cycle is τ_B (see Fig. 3C). Note that if τ_E is the time duration of an epidemic, then on an n-year cycle $\tau_B+\tau_E=n$. By Eq. (2.4), the number of susceptible S_1 at the beginning of next epidemic is:

$$S_1=S_0+\mu\tau_B. \tag{3.1}$$

However, S_0 and τ_B depend on each other, because, for example, a low value of S_0 will result in a long build-up time until the next

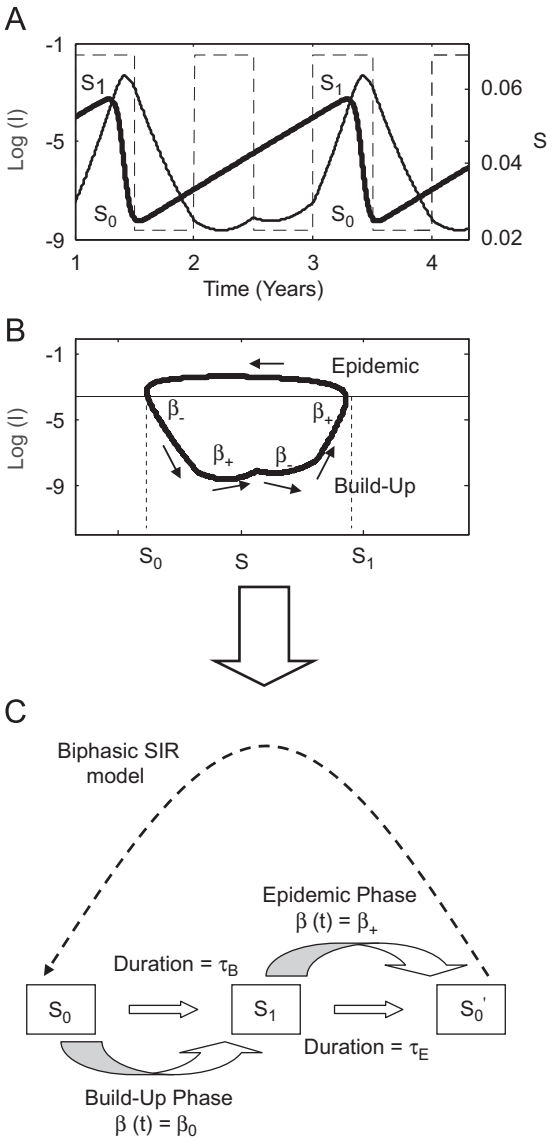

Fig. 3. Biphasic SIR model. (A) A biennial time-series example [parameters as in Fig. 2A]. (B) Phase-Plane diagram corresponding to the time-series. (C) The model approximates forced SIR limit-cycle dynamics as an alternation between two different phases. The build-up phase describes the linear build-up of susceptibles between the wake of the current epidemic (S_0) until the onset of the next epidemic (S_1). The epidemic phase, where ($\beta(t)=\beta_+$), models the fall of susceptible between S_1 to S'_0 at the conclusion of next epidemic. Note that on a limit-cycle the summed durations of the build-up time (τ_B) and the epidemic time (τ_E) is n years (n integer), the period of the limit-cycle.

epidemic; their relationship is (see Methods):

$$S_0(\tau_B)=\frac{1}{R_0}-\frac{\mu}{2}\tau_B, \tag{3.2}$$

Eq. (3.1) thus gives

$$S_1=\frac{1}{R_0}+\frac{\mu}{2}\tau_B. \tag{3.3}$$

Note here that S_1 is not dependent on the strength of seasonality δ. This is because during the build-up phase δ has little net effect on infectives, and setting $\beta(t)=\beta_0$ proves to be a good approximation in this regime (see Appendix A).

Consider now the epidemic phase that occurs in the following season. Because epidemics almost always occur in the Hi-Season (see Appendix B), we assume that in the epidemic phase $\beta(t)=\beta_+$, so that we obtain from (2.1)

$$\frac{dI}{dS}=-1+\frac{1}{R_0(1+\delta)S},\quad R_0\equiv\beta_0/\gamma, \tag{3.4}$$

where $R_0(1+\delta)$ might be considered the "basic reproductive ratio" of the Hi-Season (see Bacaër and Ait Dads (2011), for a criticism of the concept of 'time-dependent reproductive ratio'). The solution of (3.4) is (see also Bacaër and Gomes (2009) for a study of the final epidemic size in the periodic SIR model without demography)

$$I(S)=-S+\frac{Ln(S)}{R_0(1+\delta)}+const. \tag{3.5}$$

If the epidemic starts and ends with a very small number of infectives, then (Eq. 3.5) yields a relationship between the suceptibles S_1 at the initiation of the epidemic and the number S'_0 at the end of the epidemic phase:

$$\exp\left[R_0(1+\delta)(S_1-S'_0)\right]=\frac{S_1}{S'_0}, \tag{3.6}$$

Since the model dynamics is periodic, we enforce the condition $S_0'=S_0$ in (3.6). Inserting Eqs (3.1)–(3.3) into (3.6), gives:

$$\exp[R_0(1+\delta_c)\mu\tau_B]=(2+R_0\mu\tau_B)/(2-R_0\mu\tau_B), \tag{3.7}$$

where δ_c is the required strength of the seasonality to form an n-year limit cycle. If ($R_0\mu\tau_B<1.5$), δ_c can to a good approximation be taken as (see Methods):

$$\delta_c\approx\frac{(R_0\mu\tau_B)^2}{12}. \tag{3.8}$$

The equation describes how δ_c depends on R_0 ($=\beta_0/\gamma$) and μ for an n-year cycle. That is, assume a spread-of-disease dynamics described by the parameters R_0 and μ, and that τ_B (with $\tau_B+\tau_e=n$) is the duration in which there is susceptible build-up from S_0 at the wake of the current epidemic to S_1 at the onset of the next epidemic. Then, the epidemic transmission-rate $\beta_+\equiv\beta_0(1+\delta_c)$ defines an epidemic that maps S_1 back exactly to S_0 thereby "closing the cycle."

Note that a δ below δ_c would lead to a build-up time shorter than τ_B, and would consequently correspond to a cycle shorter than n years. δ_c thus acts as a bifurcation-point threshold where the dynamics of the forced SIR model changes from period $n-1$ to period n as δ increases above δ_c. To make things more concrete, we focus on the case of a transition from biennial to annual dynamics. This transition is important from a predictive point of view, as it might imply an epidemic in the coming year. The model bifurcation values for δ, as a function of R_0 and μ, are shown in Fig.4. The bifurcation values depend on τ_B and it is reasonable, as an initial first approximation, to set $\tau_B\simeq 2$. The justification here is that for realistic parameters values the outbreak is extremely fast compared to the buildup time which is approximately two years. Fig. 4A shows that the model threshold predictions in this case ($\tau_B\simeq 2$) are in reasonable agreement with SIR simulations. However, the model results can be significantly improved if we take advantage of the fact that epidemics often occur over several months, rather than the zero time approximation used above. We have found that $\tau_B=1.7$ years gives an excellent fit when predicting the bifurcation transition from annual to biennial as shown in Fig. 4B. Importantly, in Appendix C, we show that it is possible to obtain a theoretical estimate of the epidemic time, and thus of τ_B, based solely on the

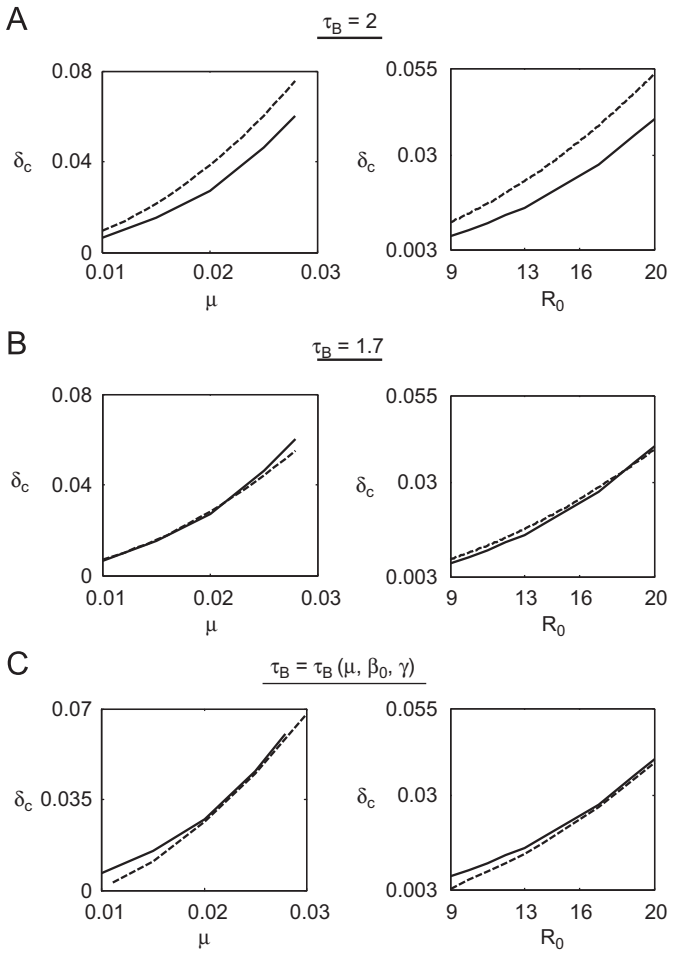

Fig. 4. SIR simulations (full line) vs. analytical results given by Eq. (3.8) (dashed line), for bifurcation values of biennial to annual transition. Bifurcation values of δ_c are plotted as a function of μ (left panel) with $R_0=17$, and as a function of R_0 (right panel) with $\mu=0.02$ years^{-1}. Note $R_0=\beta_0/\gamma$, with γ fixed in these simulations to 66 years^{-1}. (A) Analytical results with $\tau_B=2$ years. (B) Analytical results with $\tau_B=1.7$ years. (C) Analytical results with τ_B calculated from the model parameters $\{\mu, \beta_0, \gamma\}$ (see Appendix C).

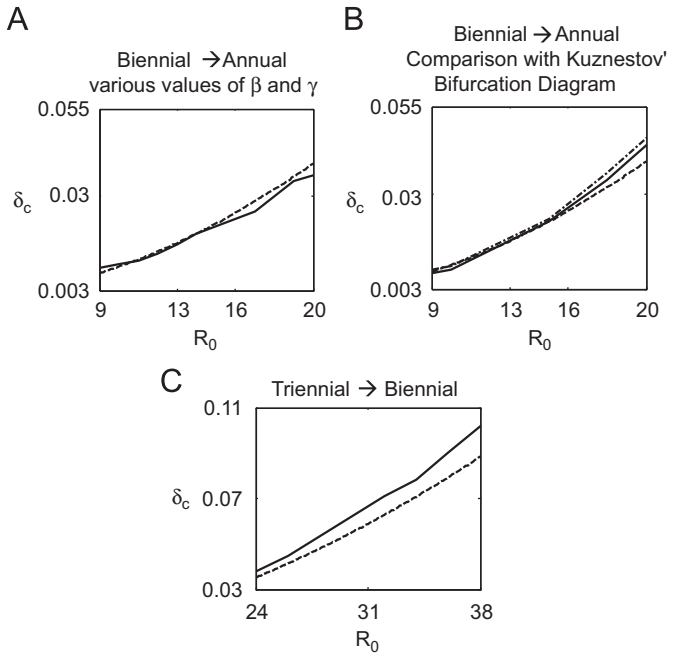

Fig. 5. SIR simulations (full line) vs. analytical results given by Eq. (3.8) (dashed line), for bifurcation values. (A) Bifurcation values of δ_c for biennial to annual transition are plotted as a function of R_0 with $\mu=0.02$ years^{-1}. $\tau_B=1.7$ years. Different γ's were used here, and values are presented as $[R_0, \gamma]$ (note γ in units year^{-1}): [(9,161)]; [(11,132)]; [(12,121)]; [(13,111.7)]; [(14,104)]; [(17,42.7)]; [19,38.2]; [20,36.3]. (B) Same as (A) but here γ is fixed to 100 years^{-1}. The dashed-dotted line shows the values extracted from Kuznestov and Piccardi's (1994) bifurcation diagram. (C) Bifurcation values of δ_c for triennial to biennial transition are plotted as a function of R_0 with γ fixed to 66 years^{-1} and with $\mu=0.02$ years^{-1}. $\tau_B=2.7$ years.

model parameters alone (i.e., R_0 and μ). In Fig. 4C, we present results where we use these estimates to determine the bifurcation values of δ and again find them to be in agreement with SIR simulations. To further examine the model, we show in Fig. 5A that, in accord with the bifurcation equation (Eq. (3.8)), our model prediction scales as a function of the ratio β/γ ($=R_0$) for different regimes of both β and γ, rather than as a function of each of these parameters separately. Because our model is only approximate, switching from one regime to other results in the wavy fit to the simulation results. We also demonstrate the model bifurcation predictions are in good agreement with the well documented bifurcation diagram of Kuznestov and Piccardi's (1994), where they considered $\gamma=100$ and $\mu=0.02$ (Fig. 5B, we examined a slice of the bifurcation diagram). Last, we tested the model predictions for higher-order cycles, specifically, for triennial to biennial transitions (Fig. 5C). It is apparent that in these cases as well, the model predictions for δ_c as a function of R_0 are in very good accord with the simulations.

Importantly, the bifurcation equation (Eq. (3.8)) suggests that the epidemiological parameters R_0 and μ control the epidemic frequency. For example, consider biennial epidemics dynamics such that δ is above the biennial transition point, i.e., $\delta > \delta_c$. Then a sufficient increase in either R_0 or μ (with no change in δ) will reverse the inequality yielding $\delta < \delta_c$ and, consequently, give rise to annual epidemics. (Note that our argument depends on the assumption that τ_B in [Eq. (3.8)] is not dependent or at most weakly dependent on R_0 and μ, as we show in Appendix C.)

3. Discussion

The forced SIR model is one of the simplest models for describing infectious disease epidemics, and yet, despite many attempts in the past, is almost impossible to solve analytically. To overcome this problem, we developed the B-SIR model, which approximates the dynamics of the forced SIR model on a limit cycle. B-SIR model describes well the SIR dynamics for the range of parameters that corresponds to childhood infectious diseases such as measles (i.e., $R_0=10\ldots 20$, $\mu=0.01\ldots 0.03$) (Anderson and May, 1991; Keeling and Rohani, 2007). The analysis of the B-SIR model yielded a simple equation (Eq. (3.8)) that predicts well the scaling of the bifurcation point from annual to biennial dynamics as a function of key epidemiological parameters. The analytically predicted bifurcation values closely match results obtained from the forced SIR simulations (Figs. 4 and 5).

It is interesting to remark here that recently Andreasen (2003) has obtained analytical predictions of the bifurcation point for a forced SIRS model. The SIRS model differs from the SIR in that recovered individuals gain only short-time immunity against the infection and may become susceptible again. However, Andreasen (2003) did not attempt to incorporate seasonal forcing and the transmission rate was assumed constant throughout the year in that model. To the best of our knowledge, the bifurcation equation presented in this work (Eq. (3.8)) is the first derivation for a *seasonally* forced epidemiological model.

The bifurcation equation (Eq. (3.8)) makes it possible to predict the effect of key epidemiological parameters on the average time τ between epidemics. For example, the equation predicts that a relatively high δ will drive dynamics into a regime where epidemics occur every two or more years ($\tau >=2$) rather than annually ($\tau=1$). This is because a high infection rate β_+ (corresponding to a high δ) during an epidemic will drive susceptibles to a level that is below the critical value S_c, and thus will result in a 'skip'. The equation also states that a large enough increase in the birth rate-constant μ will lead to annual dynamics. Intuitively, a large enough birth-rate μ ensures that shortly after an outbreak there will be enough newborn susceptibles to make possible yet another epidemic. Last, the equation implies that a large R_0 will result in annual epidemic dynamics. Remarkably, this effect could not be obtained by simple reasoning because an increase in R_0 seems to either increase or decrease τ depending on whether the susceptible build-up phase or epidemic phase is considered, respectively. For example, if R_0 is large then at the end of an epidemic susceptibles will almost be depleted and the susceptible build-up time is expected to last longer; on the other hand, during the build-up phase an elevated R_0 would decrease the duration until the epidemic threshold $R_0*S=1$ is crossed, i.e., it would *shorten* the time until the next epidemic.

The bifurcation equation (Eq. (3.8)) thus allows to understand trends that have been observed via analytical and numerical studies by other researches: (i) there is a shift from annual to multiennial dynamics as δ increases and as either μ or R_0 decreases (Earn et al., 2000; Keeling et al., 2001; Ferrari et al., 2008; Keeling and Rohani, 2007; Nguyen and Rohani, 2008) (ii) the bifurcation point scales in an identical manner with β and μ (Conlan and Grenfell, 2007). It should be noted, however, that the SIR model has a complex bifurcation diagram and there are regimes where multiple attractors coexist (see, e.g., Kuznestov and Piccardi's, 1994; Earn et al., 2000). Thus, while we correctly predict the annual to biennial bifurcation point, the actual switching to the biennial regime may be influenced by the presence of another coexisting attractor. That is to say, the particular initial conditions and the presence of stochasticity can play a role, and not just the passing through a bifurcation point.

Importantly, the effects inferred from (Eq. (3.8)) are also in accordance with empirical epidemiological observations. Previous analyses have shown that in the pre-vaccination era, the increase in birth-rate μ in the United States (after the great-depression) and in the United Kingdom (post world-war II baby boom), was the factor responsible for driving measles dynamics from biennial to annual oscillations (Finkenstädt and Grenfell, 1998; Earn et al., 2000; Finkenstädt and Grenfell, 2000). This is a clear prediction of (Eq. (3.8)). It was also argued (Ferrari et al., 2008) that the unusually powerful seasonality in Niger, Africa, is responsible for the irregular high amplitude measles outbreaks having all the hallmarks of chaos. Correspondingly, (Eq. (3.8)) identifies the first bifurcation in the expected period-doubling route to chaos that continues as seasonality (δ) increases. Similar erratic episodic outbreaks are typical of other strongly seasonal (high δ) systems, such as polio outbreaks in India (Grassly et al. (2006)).

The biphasic method described here can provide a powerful technique for analyzing different seasonally forced epidemiological models. A natural extension would be the study of the forced SIRS model (as opposed to the SIR model here) and could thus yield valuable insights into the dynamics of influenza, a program we are currently initiating. A better understanding of the epidemics time patterns through the methods suggested here could help foresee dynamic transitions in epidemics and, in turn, may allow advanced preparation for suitable measures that might be required.

4. Methods

4.1. Biphasic SIR (B-SIR) model

The dynamics of the SIR model may be visualized in the S-Log(I) phase-plane (Fig. 2). It should be noted that the (dS/dt) null-cline separates between the build-up phase and the epidemic phase (Olinky et al., 2008). We separately approximate the SIR dynamics in the build-up and epidemic phases, and then combine these approximations to yield the B-SIR model.

4.2. Build-up dynamics

During the build-up phase seasonality has little influence on the dynamics because in the low season δ acts to decrease the number of infectives by almost the same amount it increases infectives in the following high season, so that to a good approximation $\beta(t)=\beta_0$ (Appendix A). In addition, we take into account that in the parameters regime of interest: (1) $I \ll (\mu/S\beta^{\pm})$ (2) $S_0 \ll 1$ and (3) $[\mu t] \ll 1$ (the latter inequality holds because for human population $\mu < 0.02$ and recurrent epidemics are assumed to be a period of only few years). The seasonally forced SIR model can thus be approximated in the build-up phase as:

$$\frac{dW}{dt} = \beta_0 S - \gamma; \quad S(t) = S_0 + \mu t. \tag{4.1}$$

where $W=\ln(I)$. Note above that for dW/dt we ignored μ since, in our parameters regime, $\mu \ll \gamma$. Integration of this equation yields

$$W(t) = W_0 + \beta_0 \mu t^2/2 + (\beta_0 S_0 - \gamma)t. \tag{4.2}$$

The B-SIR model assumes that dS/dt null-cline is almost parallel to the S axis (Fig. 1), so that we can approximate $\log(I)$ to have the same value when susceptibles reach S_0 and S_1 (Olinky et al., 2008). The time τ_B required for the build-up is obtained by setting $W(t)=W_0$ (a consequence of the assumption that dS/dt null-cline is parallel to S-axis). The result is

$$\tau_B = \frac{2}{\mu}\left(\frac{1}{R_0} - S_0\right); \quad R_0 \equiv \beta_0/\gamma. \tag{4.3}$$

Therefore, starting with S_0 at the very beginning of the build-up phase, S_1 at the end of the phase is approximated by Eq. (2.1) as

$$S_1 = S_0 + \mu\tau_B = S_0 + 2\left(\frac{1}{R_0} - S_0\right). \tag{4.4}$$

4.3. Epidemic dynamics

S'_0 at the end of the current epidemic, is related to S_1 at the end of the previous epidemic by Eq. (3.4)

$$\exp\left[R_0(1+\delta)(S_1 - S'_0)\right] = \frac{S_1}{S'_0}. \tag{4.5}$$

4.4. Periodic solution

Note that since S_1 depends on S_0 (see Eq. (4.4)), Eq. (4.5) describes a map from S just after one season epidemic (S_0) to S just after following season epidemic (S'_0). We calculate the map for periodic dynamics by setting $S'_0=S_0$ in (Eq. (4.5)) and obtain:

$$\exp[R_0(1+\delta_c)\mu\tau_B] = 1 + 2R_0\mu\tau_B/(2 - R_0\mu\tau_B), \tag{4.6}$$

where δ_c is the strength of seasonality that enforces a cycle. For $R_0\mu\tau < 1.5$, the equation can to a good approximation be solved

for δ_c (we expand in a Taylor series $Ln(2+x/2-x)$, around $x=0$, where $x \equiv R_0\mu\tau_B$):

$$\delta_c = \frac{Ln[1+2R_0\mu\tau_B/(2-R_0\mu\tau_B)]}{R_0\mu\tau_B} - 1 \approx \frac{(R_0\mu\tau_B)^2}{12}. \quad (4.7)$$

Acknowledgments

We gratefully acknowledge the support of EU-FP7 grant Epiwork, the Israel Science Foundation and the Israel Ministry of Health.

Appendix A. Effect of seasonality in the build-up phase

We show below that during the build-up phase seasonality has little influence on the dynamics, so that to a good approximation we can set $\beta(t)=\beta_0$.

Taking into account that in the parameters regime of interest, $S(t) \ll 1$ and $I \ll (\mu/S\beta^{\pm})$, the seasonally forced SIR model can be approximated in the build-up phase as (refer Eq. (2.4) in main text, and note $\mu \ll \gamma$, so that $[\mu+\gamma] \approx \gamma$):

$$\frac{dW}{dt} = \beta(t)S - \gamma; \quad S(t) = S_0 + \mu t. \quad (A.1)$$

where $W=\ln(I)$, and S_0 is the number of susceptibles at the initiation of the build-up phase. Following Olinky et al. (2008), integration of this equation yields

$$W(t) - W_0 = -\gamma(t-t_0) + \int_{t_0}^{t} \beta(t)(S_0+\mu t)\,dt, \quad (A.2)$$

where W_0 is the value of W at the initiation of the build-up phase. If we assume that the build-phase starts at $t_0=0$ with the *Lo*–season, and denote W_1, W_2 as the values of W at the time points where the season changes *Lo*- > *Hi* and *Hi*→*Lo*, respectively, one obtains (recall each season lasts for half a year):

$$W_1 - W_0 = \frac{1}{2}\left\{-\gamma + \beta_0(1-\delta)\left([S_0] + \frac{1}{4}\mu\right)\right\}, \quad (A.3)$$

$$W_2 - W_1 = \frac{1}{2}\left\{-\gamma + \beta_0(1+\delta)\left(\left[S_0 + \frac{1}{2}\mu\right] + \frac{3}{4}\mu\right)\right\}, \quad (A.4)$$

So that after two seasonal changes the increase in W is:

$$W_2 - W_0 = \left\{-\gamma + \beta_0\left(S_0 + \frac{3}{2}\frac{\mu}{2} + \delta\frac{\mu}{2}\right)\right\}, \quad (A.5)$$

Note the contributions $-\delta S_0$ in (W_1-W_0) and $+\delta S_0$ in (W_2-W_1) cancel out. Moreover, terms of order $\delta\mu$ are relatively small in the parameter ranges we use, and can therefore be neglected. This is an important result suggesting that to first order, the change in I and S during the build-up phase, can be calculated by setting $\beta(t)=\beta_0$.

Consider now a biennial or higher-order cycle, where the build-up time lasts more than one year (two-seasons). It can be seen, by dividing the total build-up time into sequences of seasons, that the effect of seasonality tends to cancel out every two seasons, and consequently has a minor impact on the dynamics. It should be remarked, however, that our analysis assumed that the change *Hi*- > *Lo* always starts at the initiation of the build-up phase, and that the build-up time lasts an integral number of years. A more rigorous analysis that excludes these restrictions/assumptions still shows the effect of seasonality is small and in practice negligible. The reason being, the total build-up time is generally evenly split between the Hi and the Lo seasons.

Appendix B. The synchrony effect

Numerical simulations identify an important characteristic of the SIR model dynamics near the bifurcation point that separates biennial and annual regimes. Close to the point of bifurcation biennial cycles synchronize with the seasonal change in that the susceptibles peak at the time when there is a change from *Lo* to *Hi* season (Fig. A1). This synchronization fades for parameters values away from the bifurcation point (Fig. A1). The synchronization phenomenon is found for a wide range of parameters setups when close to the bifurcation point. The B-SIR model we present is a simplification of the SIR model. In particular, it makes use of the synchrony effect by assuming that the *initiation* of the epidemic phase (previously defined in this work as the point where suceptibles peak (see Fig. 2)), *coincides* with the onset of the *Hi* season (Eq. 3.4).

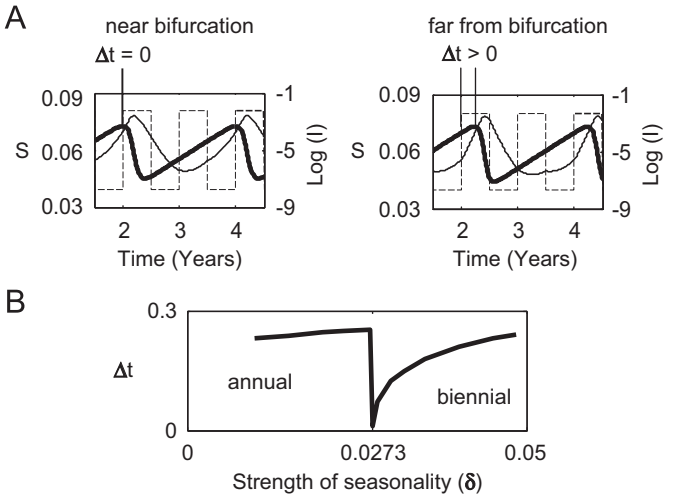

Fig. A1. Synchrony effect near bifurcation. (A) The left panel shows the time series of S (thick line), $\log[I]$ (thin line) and $\beta[t]$ (dashed line) for a biennial limit-cycle just above the bifurcation point ($\delta=0.0273$). Note that initiation of the *Hi* season coincides ($\Delta t=0$) with the peak of susceptibles. The right panel shows time series of simulations where δ is further away from the bifurcation point, $\delta=0.0485$, and it is apparent that the *Hi* season starts well *before* the sucpetibles peak. In these simulations $\beta_0=1122$ per year, $\gamma=66$ per year, $\mu=0.02$ per year. (B) Forced SIR simulations results for the the time-difference between the initiation of the *Hi*-season and the peak of susceptibles, as function of δ. Note the synchrony is manifested only close to the bifurcation point at $\delta \approx 0.0273$. Parameters-setup as in (A).

Appendix C. Calculation of build-up time

Here we use the unforced SIR model

$$\frac{dS}{dt} = \mu(1-S) - \beta IS, \quad \frac{dI}{dt} = \beta IS - (\gamma+\mu)I$$

to calculate an estimate for τ_B from the model parameters R_0 and μ.

It has been previously shown (Katriel and Stone, 2010) that a good estimate of the epidemic time τ_E can be obtained from a knowledge of R_0 and of the number of susceptible S_1 at the initiation of an epidemic:

$$\tau_E = \frac{1}{\gamma}\int_{\alpha Z/(1-Z)^{-\alpha}-1}^{\alpha Z/1-(1-Z)^{\alpha}} \frac{1}{u}\frac{du}{R_0 S_1(1-u)+\log(u)} \quad (C.1)$$

In this formula, γ is the recovery rate from infection. α defines the duration of the epidemic as the time from epidemic onset until the fraction α of the maximum possible new infectives cases occur (the maximum number is obtained in the limit of epidemic

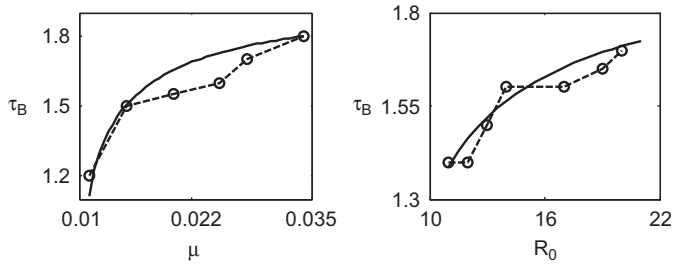

Fig. A2. SIR simulations (dashed line) vs. theoretical estimates given by Eq. (C4) (full line), for the build-up time τ_B on a biennial cycle. Values of τ_B are plotted as a function of μ (left panel) with $R_0=17$, and as a function of R_0 (right panel) with $\mu=0.02$ years^{-1}. Note $R_0=\beta_0/\gamma$, with γ fixed in these simulations to 66 years^{-1}.

time goes to infinity); α is set (Katriel and Stone, 2010) to 0.9. Z is a solution of the implicit equation $1-Z=e^{-R_0S_1Z}$.

We denote the function (A.1) for τ_E as f_E:

$$\tau_E=f_E(R_0,S_1) \tag{C.2}$$

However we showed above (Eq. 3.3 in the main text) that S_1 depends on R_0, μ and on the build-up time τ_B

$$S_1=\frac{1}{R_0}+\frac{\mu}{2}\tau_B, \tag{C.3}$$

so that we rewrite (C.2) on an *n-year* cycle as

$$n-\tau_B(n)=f_E(R_0,\mu,\tau_B(n)), \tag{C.4}$$

where $\tau_B(n)$ is the build-up time on an n-year cycle. The build-up time can thus be obtained by numerically solving (C.4) for τ_B. In (Fig. A2) we show the theoretical estimations for $\tau_B(2)$ as a function of R_0 and μ are in close agreement with SIR simulations. Importantly, we remark here that $\tau_B(2)$ is a slowly increasing function of R_0 and μ (Fig. A2), and does not substantially affect the trend between δ_c and the variables R_0 and μ (Eq. (3.8)).

References

Altizer, S., Dobson, A., Hosseini, P., Hudson, P., Pascual, M., Rohani, P., 2006. Seasonality and the dynamics of infectious diseases. Ecol. Lett. 9, 467–484.

Anderson, R.M., May, R.M., 1991. Infectious Diseases of Humans: Dynamics and Control. Oxford University Press, New York.

Andreasen, V., 2003. Dynamics of annual influenza A epidemics with immuno-selection. J. Math. Biol. 46, 504–536.

Aron, J.L., Schwartz, I.B., 1984. Seasonality and period-doubling bifurcations in an epidemic model. J. Theor. Biol. 110, 665–679.

Bacaër, N., Ait Dads, E.H., 2011. Genealogy with seasonality, the basic reproduction number, and the influenza pandemic. J. Math. Biol. 62, 741–762.

Bacaër, N., Gomes, M.G.M., 2009. On the final size of epidemics with seasonality. Bull. Math. Biol. 71, 1954–1966.

Begon, M., Telfer, S., Smith, M.J., Burthe, S., Paterson, S., Lambin, X., 2009. Seasonal host dynamics drive the timing of recurrent epidemics in a wildlife population. Proc. Biol. Sci. 276, 1603–1610.

Bolker, B.M., Grenfell, B.T., 1993. Chaos and biological complexity in measles dynamics. Proc. R. Soc. Lond. B 251, 75–81.

Conlan, A.J., Grenfell, B.T., 2007. Seasonality and the persistence and invasion of measles. Proc. Biol. Sci. 274, 1133–1141.

Earn, D.J., Rohani, P., Bolker, B.M., Grenfell, B.T., 2000. A simple model for complex dynamical transitions in epidemics. Science 287, 667–670.

Ferrari, M.J., et al., 2008. The dynamics of measles in sub-Saharan Africa. Nature 451, 679–684.

Fine, P.E., Clarkson, J.A., 1982. Measles in England and Wales—I: An Analysis of Factors Underlying Seasonal Patterns. Int. J. Epidemiol. 11, 5–14.

Fine, P.E., Clarkson, J.A., 1986. Seasonal Influences on Pertussis. Int. J. Epidemiol. 15, 237–247.

Finkenstädt, B.F., Grenfell, B.T., 1998. Empirical determinants of measles metapopulation dynamics in England and Wales. Proc. Roy. Soc. B 265, 211–220.

Finkenstädt, B.F., Grenfell, B.T., 2000. Time series modelling of childhood diseases: a dynamical system approach. Appl. Stat 49, 187–205.

Finkenstädt, B.F., Keeling, M., Grenfell, B.T., 1998. Patterns of density dependence in measles dynamics. Proc. R. Soc. Lond. B 265, 753–762.

Grassly, N.C., Fraser, C., Wenger, J., Deshpande, J.M., Sutter, R.W., Heymann, D.L., Aylward, R.B., 2006. New strategies for the elimination of polio from India. Science 314, 1150–1153.

Grossman, Z., Gumowski, I., Dietz, K.,1977. The incidence of infectious diseases under the influence of seasonal fluctuations—analytical approach. In: Nonlinear Systems and Applications, pp.525–546.

Katriel, G., Stone, L., 2010. Pandemic dynamics and the breakdown of herd immunity. PLoS One 5, e9565.

Keeling, M., Rohani, P., Grenfell, B.T., 2001. Seasonally forced disease dynamics explored as switching between attractors. Physica D 148, 317–335.

Keeling, M.J., Rohani, P., 2007. Modeling Infectious Diseases in Humans and Animals (Chapters 1,2,5). Princeton University Press.

Kermack, W.O., McKendrick, A.G., 1927. Contributions to the mathematical theory of epidemics. Proc. Roy. Soc. A 115, 700–721.

Kuznestov, Yu.A., Piccardi, C., 1994. Bifurcation analysis of periodic SEIR and SIR epidemic models. J. Math. Biol. 32, 109–121. (Figure 3 therein).

London, W.P., Yorke, J.A., 1973. Recurrent outbreaks of measles, chickenpox and mumps. 1. Seasonal variation in contact rates. Am. J. Epidemiol. 98, 453–468.

measdata.html-〈http://www.zoology.ufl.edu/bolker/measdata.html〉.

Nguyen, H.T., Rohani, P., 2008. Noise, nonlinearity and seasonality: the epidemics of whooping cough revisited. J. R. Soc. Interface 5, 403–413.

Olinky, R., Huppert, A., Stone, L., 2008. Seasonal dynamics and thresholds governing recurrent epidemics. J. Math. Biol. 56, 827–839.

Olsen, L.F., Schaffer, W.M., 1990. Chaos versus noisy periodicity: alternative hypotheses for childhood epidemics. Science 249, 499–504.

Pascual, M., Dobson, A., 2005. Seasonal patterns of infectious diseases. PLoS Med. 2, 18–19.

Sharma, D.C., 2003. WHO to strengthen commitment to polio eradication. Lancet 362, 454.

Smith, H.L., 1983. Subharmonic bifurcation in an S-I-R epidemic model. J. Math. Biol. 17, 163–177.

Stone, L., Olinky, R., Huppert, A., 2007. Seasonal dynamics of recurrent epidemics. Nature 446, 533–536.

Trevelyan, B., Smallman-Raynor, M., Cliff, A.D., 2005. The spatial dynamics of poliomyelitis in the United States: from epidemic emergence to vaccine-induced retreat, 1910–1971. Ann. Assoc. Am. Geogr. 95, 269–293.

Ward, R., 1944. The epidemiology of poliomyelitis. Bone Joint Surg. Am 26, 829–832.